Journal of *Marine Science and Engineering*

MDPI

Article

Strike-Slip Activity of the Tinjar–West Baram Fault in the Southern South China Sea: Implications for Sedimentation in the Zengmu Basin and Hydrocarbon System

Kunsheng Qiang * and Guangxue Zhang

Guangzhou Marine Geological Survey, Guangzhou 511458, China
* Correspondence: qks80@163.com

Abstract

The Tinjar–West Baram Fault in the southern South China Sea is a major NW-trending strike-slip fault that has remained tectonically active since the Oligocene. It forms a key structural boundary between the Zengmu, Beikang, and Nansha Trough basins. Multiphase strike-slip movements have strongly controlled sediment provenance dispersal pathways, and reservoir development in the Zengmu Basin, yet the sedimentary response to these tectonic processes remains poorly understood. This study integrates 2D seismic profiles to analyze the fault geometry, kinematics, and impact on deep-water sedimentary systems. Results indicate that Oligocene right-lateral motion directed sediment supply from the southwest, mainly sourced from Kalimantan, forming fluvial–deltaic systems with depocenters in the southern basin. Since the Late Miocene, a transition to left-lateral motion reoriented sediment provenance toward the southeast, leading to delta-front complexes and northward migration of depocenters. Strike-slip activity deformation enhanced rock fragmentation and sediment supply, producing fan delta, fluvial, and shallow lacustrine facies near the fault. Associated uplift and subsidence induced relative sea-level fluctuations, resulting in alternating transgressive–regressive sequences. From the Late Eocene to Miocene, the basin evolved from a land–sea transitional system to a deltaic–carbonate complex controlled by the paleo-Sunda River. During the Pliocene–Quaternary, sedimentation was dominated by shallow-marine shelf and semi-deep-marine deposits. Fault-related fracturing significantly enhanced porosity and permeability, creating favorable conditions for hydrocarbon migration and entrapment in both sandstone and carbonate reservoirs. These findings demonstrate a strong coupling between strike-slip fault activity and sedimentary system evolution, providing important insights into sedimentary processes and hydrocarbon potential in strike-slip fault-bounded basins globally.

Keywords: sedimentary control; strike-slip activity; Tinjar–West Baram Fault Zone; Zengmu Basin; southern South China Sea

Check for updates

Academic Editors: Mianmo Meng, Wenming Ji and Guodong Cui

Received: 8 December 2025
Revised: 7 February 2026
Accepted: 12 February 2026
Published: 4 March 2026

Copyright: © 2026 by the authors. Licensee MDPI, Basel, Switzerland. This article is an open access article distributed under the terms and conditions of the Creative Commons Attribution (CC BY) license.

1. Introduction

The South China Sea lies at the convergence of the Eurasian, Pacific, and Indo-Australian plates, making it the largest marginal sea in the western Pacific. Its tectonic evolution reflects the combined influence of the Tethyan and the Pacific tectonic domains [1,2], resulting in highly complex tectonic activity. Interactions among the Indochina Block, Nansha Block, and Sarawak-Sulu accretionary belt led the development of several medium- to large-scale sedimentary basins along the South China Sea margins. Although numerous

evolutionary models have been proposed [3–5], the role of the Tinjar–West Baram Fault, a major NW-trending strike-slip fault in the southern South China Sea, remains critical for understanding sedimentary patterns and hydrocarbon accumulation in the Zengmu Basin. Active since the Oligocene, the fault, which experienced right-lateral motion initially, shifted to left-lateral motion during the Late Miocene, and reverted to right-lateral motion from the Pleistocene to the present [6–9]. This complex kinematic evolution has strongly controlled basin architecture, sediment dispersal, and reservoir development.

Strike-slip activity induced differential uplift and subsidence, shaping basin paleotopography and sediment supply. Uplifted fault adjacent areas generated steep topographic gradients that enhanced erosion and supplied short-transport clastics, forming alluvial fan and fan deltas, whereas gentler slopes favored distal fluvial-deltaic systems with improved sediment sorting. During the early right-lateral phase (Oligocene–Miocene), coarse-grained deposits accumulated near steep slopes, while during the Late Miocene left-lateral phase, the depocenters migrated northward and fine-grained lacustrine or deep-marine sediments became dominant. Fault reaction also promoted the formation of structural traps through alternating extensional and compressional stress regimes, generating fault blocks and folds [10]. Secondary fault networks enhanced reservoirs connectivity, while fault zones served as vertical migration pathways for hydrocarbon accumulation in shallow traps. Changes in strike-slip direction further controlled depocenter migration. Since the Late Miocene, reversal from left-lateral to right-lateral motion shifted the sedimentary center from south to north, altering facies distribution, sediment thickness, and lithofacies transitions. These processes also regulated the spatial distribution of high-quality reservoirs through the development of structural slope breaks [11]. Despite these advances, sedimentary reservoir development under the multi-phase strike-slip regime of the Tinjar–West Baram Fault remains insufficiently understood, particularly regarding hydrocarbon accumulation patterns on either side of the fault. The Zengmu Basin and the adjacent Brunei-Sabah Basin, contain thick Neogene successions [12–14], making the fault system a key control on regional petroleum systems. Consequently, clarifying the sedimentary characteristics and hydrocarbon significance of the Tinjar–West Baram Fault in the Zengmu Basin remains a major research challenge in South China Sea studies.

2. Geological Background

The Tinjar–West Baram Fault Zone (T–WBFZ) is a major NW-trending strike-slip fault system in the southern South China Sea. It forms the structural boundary between the Nansha and Zengmu blocks and extends from the Tinjar River regions of Kalimantan northeastward into the offshore West Baram Fault. The T–WBFZ defines the southwestern margin of the South China Sea Basin and terminates the extension of the Nansha Trough. Structurally, it exerts strong control on basin development and sedimentation, as evidenced by thick Neogene accumulations in the Zengmu and Brunei basins formed through tilting and differential subsidence along the fault. This structural framework has also played a key role in hydrocarbon migration and accumulation [3,15]. The evolution of the Zengmu Basin reflects complex tectonic interactions related to the subduction and closure of the proto-South China Sea, followed by opening of the present South China Sea [16,17]. Throughout these processes, the Tinjar–West Baram Fault acted as a fundamental structural boundary controlling basin initiation, sediment infill, and hydrocarbon system development [18]. Since the Cenozoic, basin evolution can be divided into three stages: (1) Late Cretaceous–Early Eocene foreland basin subsidence; (2) Oligocene–Early Miocene strike-slip reactivation; and (3) Middle Miocene–Quaternary regional subsidence. Geographically, the Zengmu Basin is located in the southwestern offshore Nansha region, east of Natuna Island, west of the Nansha Trough, south of the Wan'an Shoal-Beikang Slope,

and north of the Beikang Basin. The basin is characterized by intense faulting accompanied by Cenozoic magmatic intrusions and volcanic activity [18]. Based on fossil assemblages, lithology, and seismic interpretation, a Cenozoic sequence stratigraphic framework has been established [19]. Seismic data identify five major unconformities (T2, T3, T4, T5, and Tg), defining five seismic sequences: T5–Tg (Lower-Middle Eocene), T4–T5 (Upper Eocene-Lower Oligocene), T4–T3 (Oligocene-Miocene), T3–T2 (Pliocene), and T2 and younger (Quaternary). Tectonic style, sedimentary architecture, and basement composition vary across the basin. The southern sector is dominated by deformed Paleogene strata and exposed basement, whereas the northern basement shows affinities with other Nansha basins. Structurally, the Zengmu Basin is subdivided into eight secondary units: Suokang Depression, Lanai Uplift, Tatau Depression, West Baram Uplift, East Baram Depression, South Kang Plateau, Kangxi Depression, and the Western Slope, with the Kangxi Depression forming the principal depocenter (Figure 1).

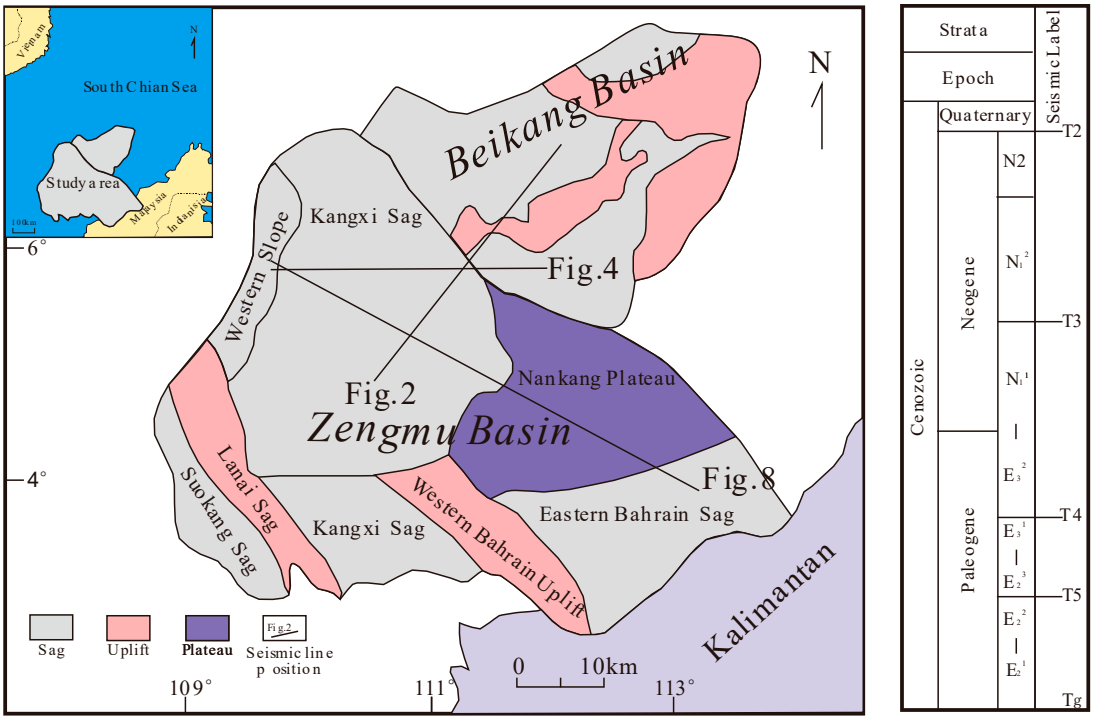


Figure 1. Tectonic and stratigraphic map of Zengmu-Beikang Basin.

The basin contains well-developed Eocene–Oligocene, Neogene, and Quaternary successions, with total sediment thickness ranging from 2000 to 11,000 m. Middle Miocene and younger deposits are typically 2000–4000 m thick, thickening northward and thinning southward [20–22].The Zengmu Basin petroleum system is characterized by Oligocene–Miocene coal-bearing strata and marine mudstones as source rocks, sandstones and carbonates as reservoirs, and mudstones and shales as seals. Sandstone reservoirs exhibit average porosities of 15–20% and permeabilities of 50–150 mD, whereas carbonate reservoirs show superior properties, with porosities of 25–30% and permeability of 300–500 mD. Hydrocarbon accumulation is controlled by both structural and depositional factors, producing diverse trap types and a characteristic "south–oil, north–gas" distribution pattern [23–25].

3. Data Sources and Methods

3.1. Multi-Channel Seismic Data Acquisition

High-resolution multi-channel seismic data were acquired by the Marine Geological 16 survey vessel of the Guangzhou Marine Geological Survey Bureau. Acquisition param-

eters included 96 receiver channels with a 25 m spacing, 24-fold coverage, a 50 m shot interval, 250 m minimum offset, 2 ms sampling rate and 7 s record length. The air-gun source had a total volume of 2821 in^3, an array length of 2625 m, a source depth of 8 m, and a streamer depth of 12 m. The survey grid spacing was approximately 40 km × 80 km.

3.2. Seismic Data Reprocessing

Seismic data were reprocessed using advanced workflows to enhance signal quality and imaging accuracy. Key steps included pre-stack multi-domain noise attenuation, multiple suppression, amplitude compensation, τ–p deconvolution, zero-phase deconvolution, complex velocity modeling in structurally complex zones, and pre-stack time migration using curved-ray algorithms. These procedures significantly improved resolution and signal-to-noise ratio enabling detailed structural and stratigraphic interpretation.

3.3. Seismic Data Interpretation

Seismic interpretation was performed using Schlumberger's GeoFrame 4.5 software platform, where an integrated interpretation database was established for horizon picking, fault mapping, and seismic–stratigraphic analysis.

4. Results and Discussion

4.1. Characteristics of the Tinjar–West Baram Fault

Seismic profiles show that the Tinjar–West Baram Fault Zone (T–WBFZ) displays classic strike-slip fault characteristics, with pronounced along-strike variations in tilting intensity that produce significant stratigraphic thickness contrasts across the fault. A prominent high-angle negative flower structure is observed, with the fault penetrating, basement rocks and vertically cutting through Cenozoic strata, forming a deeply rooted fault system. This structural architecture reflects multi-phase strike-slip activity; early right-lateral motion promoted rift basin development, whereas subsequent reactivation led to stratal tilting and depocenter migration. Marked stratigraphic contrasts across the fault include variations in thickness, orientation, and seismic facies. Fault activity also produced extensive secondary fault networks, which act, as major hydrocarbon migration pathways and control the distribution of tilted fault blocks, graben-horst structures, and associated sedimentary architectures (Figure 2).

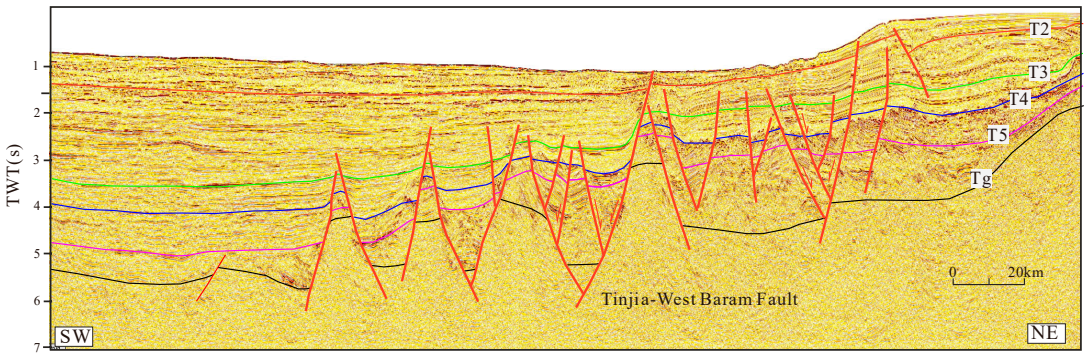


Figure 2. Cross-sectional Characteristics of the Tinjar-West Baram Fault (location shown in Figure 1).

In map view, the T–WBFZ exhibits a chevron-shaped strike-slip pattern, reflecting complex regional plate motions. This fault system controls the development of NW-trending subsidiary faults in the southern basin, which display a characteristic pattern of "northwest convergence and southeast divergence", arcuate geometries, branching structure, variable fault widths, and evidence of multi-phase deformation, highlighting the dynamic tectonic evolution of the region (Figure 3).

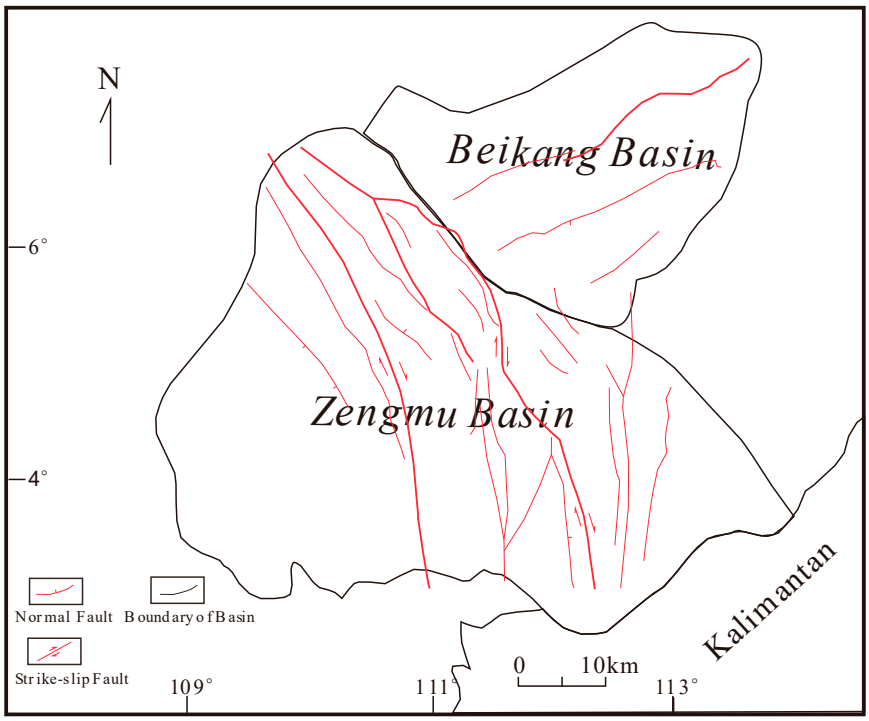


Figure 3. Fault distribution map of the Tg reflection layer.

4.2. Influence of Faulting on Sedimentary Depocenter Migration

Sedimentation and subsidence in the Zengmu Basin are primarily controlled by fault activity, with fault timing and kinematics exerting strong influence on the development and migration of sedimentary depocenters. During the Late Cretaceous Early Eocene, southward subduction of the proto-South China Sea caused basement uplift and the formation of horst–graben structures. From the Late Eocene to Late Oligocene, activation of the Tinjar–West Baram Fault Zone (T-WBTZ) initiated basin subsidence, largely governed by inherited basement faults beginning at ~23.8 Ma. By the end of the Early Miocene (~16 Ma), intensified subsidence in the southern basin established the principal depocenter. Inherited basement faults continued to control stratigraphic architecture, producing alternating zones of uplift and subsidence. During the Middle–Late Miocene (ca. 10.2–5.3 Ma), ongoing fault activity drove northward migration of the sedimentary center, accompanied by rapid sediment accumulation and continued subsidence, while most basin faults gradually became inactive. Since the Quaternary (~1.8 Ma), renewed differential subsidence, clearly imaged in seismic profiles, has further shifted the depocenter northward toward the Beikang Basin. Overall, the Zengmu Basin records a persistent south-to-north migration of sedimentary centers through time.

4.3. Influence of the Faulting on Basin Tectonic Evolution

Late Cretaceous–Eocene: During the late Maastrichtian, the Lucania Block, hosting the Zengmu Basin, was situated in northern Kalimantan. From the Paleocene to early Eocene, southwestward subduction of the proto-South China Sea beneath the Kalimantan Block caused southward drift of the Lucania Block without direct collision. By the late Eocene, continued southward motion resulted in initial collision between the southern margin of the Lucania Block and the Kalimantan accretionary complex. Basin development during this stage was primarily controlled by basement faults, including the Lupal and Bukit Mersing faults, which induced flexural subsidence and localized rifting. Subsidence was concentrated along the subduction margin, with the Nankang Platform, southwest of the Tinjar Fault, acting as the main depocenter.

Oligocene–Early Miocene: During the Oligocene, the Tinjar–West Baram Fault initiated significant strike-slip activity. Under combined compressional and strike-slip deformation, the southern Zengmu Basin became the main depocenter. In the Early Miocene, continued southward subduction of the Nansha Block beneath Sabah impeded further southward movement of the Zengmu Block, while the Tinjar–West Baram Fault exhibited pronounced dextral motion. Intensifying collision between the ucania and Kalimantan blocks led to progressive closure of the proto-South China Sea. Uplift along the southern Lucania margin formed a foreland orogenic belt, transforming regional paleogeography from "high in the north, low in the south" to "high in the south, low in the north." This uplift supplied abundant sediment to the Zengmu Basin. In the southeastern basin, NE-trending en echelon faults developed under dextral strike-slip control along the Tinjar-West Baram Fault (Figure 4). Associated fault blocks and reef complexes formed structural traps, providing favorable conditions for subsequent hydrocarbon generation and accumulation.

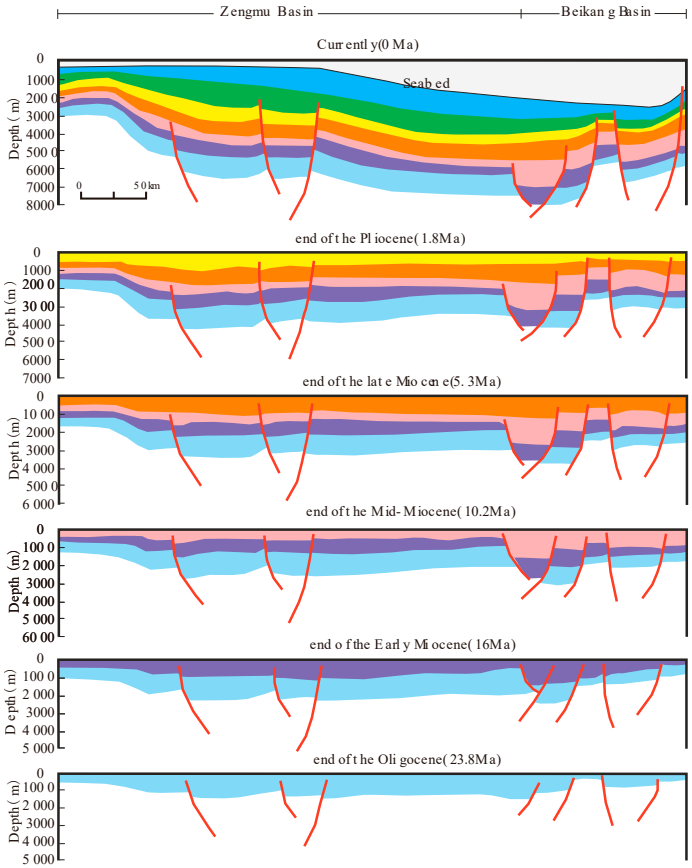


Figure 4. Cenozoic tectonic evolution profile of the Zengmu Basin (modified from [19]) (location shown in Figure 1).

4.4. Characteristics of the Sedimentary Evolution

The Zengmu Basin records a progressive sedimentary evolution closely linked to its tectonic development. Four major stages are recognized: (1) a lacustrine system during the Late Paleocene–Eocene rift stage (Tg–T5); (2) expanded lacustrine deposition during peak rifting in the Oligocene (T5–T4); (3) a deltaic–marine transgressive system during Early Miocene subsidence (T4–T3); and (4) a fully marine transgressive system from the Middle–Late Miocene to the Quaternary (T3–Q). Accordingly, the basin was successively infilled by rift-related lacustrine sediments, transitional deltaic deposits, and ultimately shallow- to semi-deep-marine sediments formed during long-term thermal subsidence (Figures 5–7). During the rift climax stage (T5–T4), rising relative sea level promoted

transitional continental-marine environments, including coastal plains, coastal swamp, shallow-marine, and semi-deep-marine settings. From the sag stage onward (T3 and younger), widespread marine transgression dominated deposition. Sediment supply was primarily derived from the Lalan River Delta to the south, prograding northward and forming extensive coastal-deltaic sequences. Continued sea-level rise shifted sedimentation toward shallow- and semi-deep-marine facies and eventually deep-marine deposits. Controlled by T3 paleogeomorphology and sediment supply variations, extensive subaqueous distributary channels, deep-water fans, and turbidite systems developed in the Beikang Basin, reflecting a mature marine depositional system under sustained thermal subsidence and high accommodation.

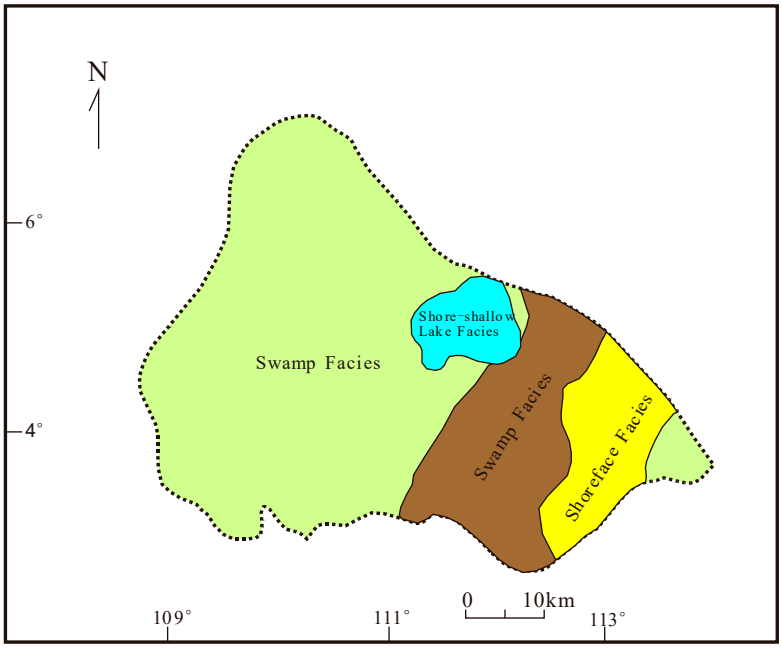


Figure 5. Planar sedimentary facies distribution map of the Zengmu Basin during the rift stage (Tg–T5).

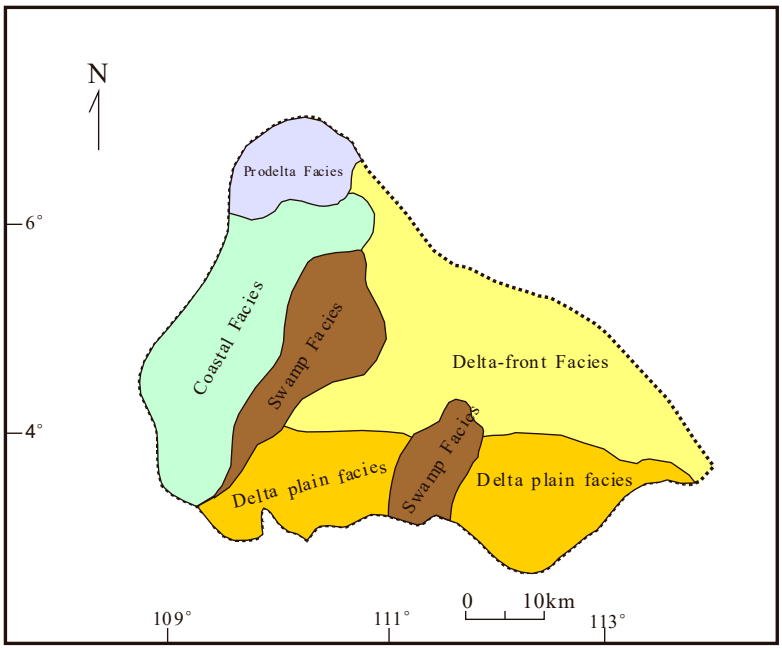


Figure 6. Sedimentary facies map of the early sag stage in the Zengmu Basin (T5–T4).

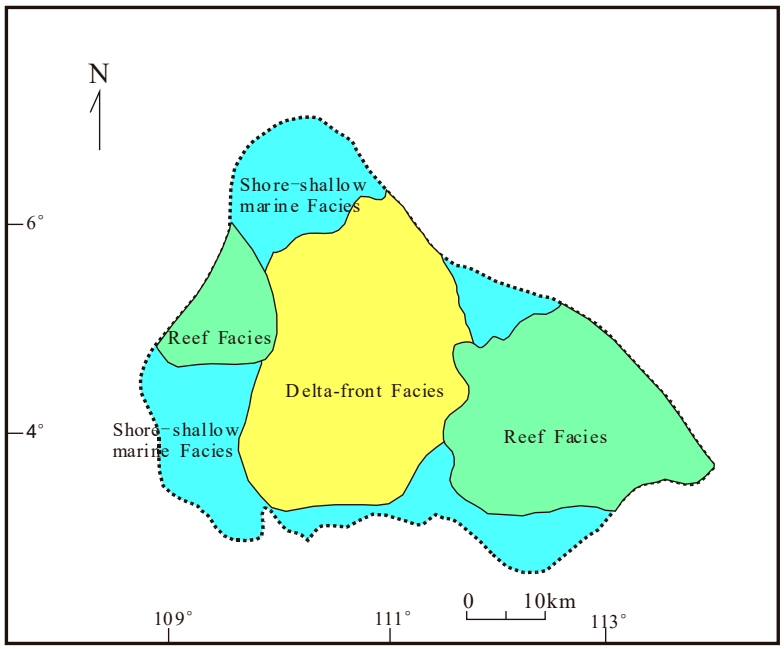


Figure 7. Sedimentary facies map of the sag stage in the Zengmu Basin (T3–Currently).

4.5. Role of Faulting in Hydrocarbon Accumulation

Fault activity has exerted a fundamental control on both Cenozoic tectonic evolution and hydrocarbon generation, migration, and accumulation in the Zengmu Basin. The principal reservoirs comprise Oligocene–Miocene sandstones and Middle–Upper Miocene limestones or reefal carbonates. Clastic reservoirs are primarily distributed in the southern uplift and East Baram Depression, whereas carbonate reservoirs are concentrated on the northern Nankang Platform and western basin slope. From the Eocene to Early Miocene, compressional tectonism related to collision between the southern basin margin and Kalimantan caused significant uplift in the southern basin, favoring the development of a self-sourced, self-reservoired, and self-sealed petroleum systems dominated by deltaic sandstones interbedded with coastal-plain and shallow-marine mudstones. During the Middle Miocene, continued strike-slip activity along the Tinjar–Sabalan Fault Zone promoted the formation of extensive carbonate platforms on the western slope and Nankang Platform, enhancing reservoir potential. Since the Late Miocene, regional thermal subsidence has dominated basin evolution, leading to deposition of thick, laterally continuous shallow- to semi-deep-marine mudstones that act as effective regional seals. Under the combined effects of collision-related compression between the Luconia Block and Kalimantan and structural deformation along the Tinjar–Sabalan Fault Zone, diverse structural traps developed, including buried hills, flower structures, fault blocks, inversion structures, and diapirs. These structures form key hydrocarbon traps and control fluid migration and accumulation. In the southern basin, compressional deformation produced fault blocks, faulted anticlines, drape folds, and rollover anticlines, which represent the dominant trap types. In contrast, reefal carbonate buildups form the primary traps on the western slope and Nankang Platform. Since the Oligocene, persistent strike-slip motion along the Tinjar–Sabalan Fault Zone has generated numerous subsidiary faults that serve as major hydrocarbon migration pathways. Early right-lateral motion enhanced vertical connectivity and fluid transport, whereas the Late Miocene transition to left-lateral motion improved fault sealing and trapping efficiency. Strike-slip intensity decreases southward, producing abundant flower structures in the northern Nankang Platform and western slope. In these areas, Oligocene–Lower Miocene source rocks are vertically linked to Middle–Upper Miocene carbonate reservoirs, forming characteristic “source–below,

reservoir–above" accumulation systems. In contrast, faults in the southern East Baram Depression became largely inactive after the Early Miocene, favoring the development of self-contained Oligocene–Lower Miocene petroleum systems (Figure 8).

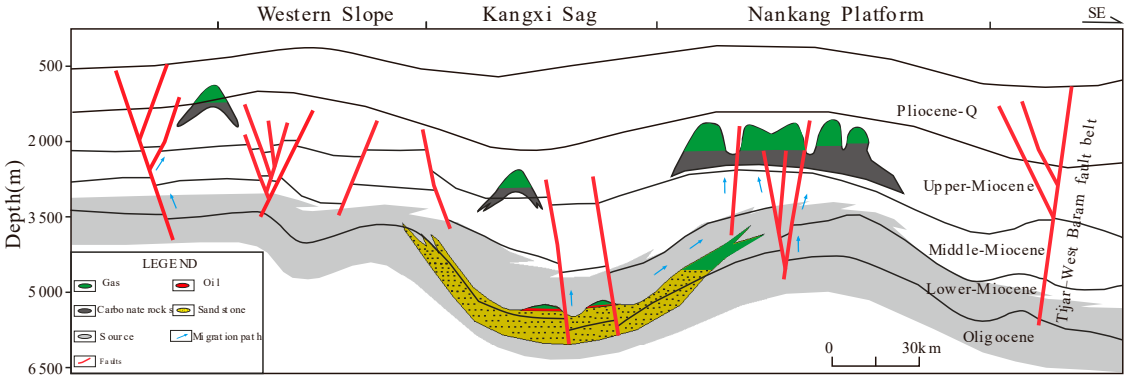


Figure 8. Hydrocarbon accumulation model of the Zengmu Basin (modified from [26]) (location shown in Figure 1).

5. Conclusions

This study area focuses on the Tinjar–West Baram Fault in the southern South China Sea, a major NW-trending strike-slip fault that defines the structural boundary between the Zengmu, Beikang, and Nansha Trough basins and has remained tectonically active since the Oligocene. Using 2D seismic profiles, this study analyzes the fault's geometry and kinematics, and assesses its control on deep-water sedimentary systems in the Zengmu Basin; this study aims to improve constraints on the sedimentary response to the fault's tectonic evolution. The main conclusions are summarized as follows:

1. Spatiotemporal Differentiation of Sedimentary Systems under Tectonic Control: Right-lateral strike-slip activity during the rifting stage exerted a primary control on basin architecture and the development of hydrocarbon "source" facies. During the Oligocene (32–25 Ma), seafloor spreading in the South China Sea induced dextral motion along the Tinjar-West Baram Fault Zone, generating extensional stress along the northwestern margin of the Zengmu Basin. This led to the formation of semi-graben depressions (e.g., the Kangxi Depression), where restricted circulation favored the deposition of organic-rich paralic carbonaceous shales and coal seams that constitute the basin's primary source rocks. More than 8 km of Cenozoic strata record intense subsidence and sediment accumulation during this phase. Differential faulting produced an asymmetric basin geometry, characterized by a steep, fault-controlled northwestern margin and a gently dipping southern slope. Proximal fan-delta systems developed along the steep margin, whereas the shallow-marine deposits sediments dominated the southeastern slope, establishing the fundamental spatial distribution of source and reservoir facies. During the Miocene (25–5 Ma), following cessation of seafloor spreading, the fault zone transitioned to left-lateral strike-slip with localized extension. This phase-controlled reservoir development and promoted southeastward depocenter migration toward the East Balingian Depression. Enhanced sediment supply related to the Sarawak Orogeny, resulted in the accumulation of thick marine mudstones (regional seals), reefal carbonate platforms (carbonate reservoirs), and deltaic to deep-water turbidite systems (clastic reservoirs). Secondary en échelon fault systems segmented the basin into a "basin–ridge" framework creating favorable structural and sedimentary conditions for hydrocarbon enrichment. Together with the thick Upper Miocene evaporites (200–500 m) and mudstone seals, a well-integrated "source–reservoir–seal" system developed, enabling vertically stacked, cross-stratal hydrocarbon accumulations involv-

ing Oligocene coal seams (gas-prone sources), Miocene sandstones and reefal limestones (reservoirs), and Pliocene mudstones (regional seals).

2. Petroleum Geological Implications of Tectono-Sedimentary Coupling: Strike-slip tectonism generated a dual-source, hydrocarbon system with contrasting thermal maturity. In the northern Kangxi Depression, shallow-water rift environments produced transitional facies source rocks dominated by Type II–III kerogen and primarily gas-prone potential. In contrast, deeper-water conditions in the southern East Balingian Depression favored the accumulation of Type I kerogen-rich marine mudstones, predominantly oil-prone [27,28]. This configuration defines a clear "southern oil–northern gas" distribution pattern. Localized mafic intrusions (e.g., diabase dikes) along the fault zone increased the geothermal gradient to ~45 °C/km, accelerating source-rock maturation and establishing the central basin as the main hydrocarbon generation center during 5–2 Ma. Strike-slip deformation produced three main trap types: (1) structural traps, including rollover anticlines, fault-blocks, and en échelon anticline clusters; (2) stratigraphic–lithologic traps, such as sandstone pinch-outs and reef–shoal carbonate buildups, and (3) compound traps combining inversion-related structures with unconformity-controlled stratigraphy. The main fault zone and its subsidiary faults form a broom-shaped fracture network that enhances vertical hydrocarbon migration (10–50 m/Ma) and locally increases reservoir permeability by 3–5 times. In compressional segments, fault gouge development and evaporite smearing improve sealing capacity, with breakthrough pressures exceeding 50 MPa.

3. Exploration Insights and Resource Potential: As a hydrocarbon-rich province in the southwestern South China Sea, the Zengmu Basin—strongly controlled by the Tinjar–West Baram Fault Zone—highlights Miocene reef-shoal complexes and strike-slip-related anticline clusters as priority exploration targets. The basin provides a representative geological model for hydrocarbon accumulation in strike-slip fault-controlled basins and offers important scientific and practical insights into tectono-sedimentary–accumulation coupling along the South China Sea plate margin.

Author Contributions: K.Q. (First Author): Methodology, Investigation, Formal Analysis, draw the drawing, Writing—Original, Draf, Response; G.Z.: Writing—Review & Editing. All authors have read and agreed to the published version of the manuscript.

Funding: National Natural Science Foundation of China (Grant No. 42130408).

Data Availability Statement: The original contributions presented in this study are included in the article. Further inquiries can be directed to the corresponding author.

Acknowledgments: We gratefully acknowledge the facilities and resources provided by the Key Laboratory of Seafloor Mineral Resources, Ministry of Natural Resources. We are also profoundly grateful to the three anonymous reviewers for their perceptive, thoughtful remarks and selfless guidance. Their incisive feedback and generous assistance have elevated this manuscript to a far higher standard, and for this, we offer our sincerest thanks.

Conflicts of Interest: The authors declare no conflict of interest.

References

1. Liao, X. Tectonic division of the pre-Cenozoic basement of the South China Sea in earth monitoring. *Phys. Chem. Earth Parts A/B/C* **2023**, *131*, 103431. [CrossRef]
2. Wang, C.; Cui, H.; Chiang, C.S.; Su, M.; Zeng, L.; Jia, J.; Wei, L. Regional detrital zircon record of the drainage sediments surrounding the South China Sea: Provenance signature and tectonic implications. *Earth-Sci. Rev.* **2024**, *258*, 104953. [CrossRef]
3. Cullen, A. Nature and significance of the West Baram and Tinjar Lines, NW Borneo. *Mar. Pet. Geol.* **2014**, *51*, 197–209. Reprint in *Mar. Pet. Geol.* **2014**, *58*, 674–686. https://doi.org/10.1016/j.marpetgeo.2014.01.009. [CrossRef]

4. Adepehin, E.J.; Bankole, O.M.; Arifin, M.H. Poro-perm evolution in Oligo-Miocene coastal sandstones: Constraining the relative influence of sedimentary facies, mineralogy, and diagenesis on analogue reservoir quality of the Nyalau Formation, Borneo. *Mar. Pet. Geol.* **2022**, *139*, 105589. [CrossRef]
5. Zhang, G. Theory of deepwater hydrocarbon accumulation controlled by progressive tectonic cycles of marginal sea in the South China Sea. *Acta Pet. Sin.* **2023**, *44*, 569–582. [CrossRef]
6. Mathew, M.J.; Menier, D.; Siddiqui, N.; Ramkumar, M.; Santosh, M.; Kumar, S.; Hassaan, M. Drainage basin and topographic analysis of a tropical landscape: Insights into surface and tectonic processes in northern Borneo. *J. Asian Earth Sci.* **2016**, *124*, 14–27. [CrossRef]
7. Tang, W.; Xie, X.J.; Wang, Y.B.; Xiong, L.Q.; Guo, J.; Li, X. Evolution of Cenozoic sedimentary architecture in Central and Southern South China Sea basins. *J. Palaeogeogr.* **2024**, *13*, 35–53. [CrossRef]
8. Jamaludin, S.N. Quantitative geo-history analysis of the Luconia-Balingian provinces, Malaysia with emphasis on the tectonic subsidence signatures. *Mar. Pet. Geol.* **2025**, *173*, 107224. [CrossRef]
9. Meng, M.; Li, Z.; Hong, Z.; Bao, J.; Jiang, Q. Quantifying pore size distribution by nuclear magnetic resonance method in tight sandstones: Comparison between water-wet and oil-wet saturated fluids. *Int. J. Hydrogen Energy* **2026**, *197*, 152608. [CrossRef]
10. Syafiq, H.; Shah, A.A.; Rachman, M.G. Shuttle radar topography-based analysis reveals the active Borneo Island Fault in Borneo, SE Asia. *J. Asian Earth Sci. X* **2024**, *12*, 100184. [CrossRef]
11. Breitfeld, H.T.; Hennig-Breitfeld, J.; Anthony, G.; BouDagher-Fadel, M.; Vermeesch, P.; Lünsdorf, K.; Rösel, D.; Schmolke, K.; Gilbricht, S. The onshore West Baram Delta deposits: Provenance and drainage in the Middle Miocene to Pliocene in NW Borneo and comparison to the Champion Delta. *Mar. Pet. Geol.* **2023**, *158*, 106537. [CrossRef]
12. Zhu, C.; Tang, W.; Yin, Y.; Song, S.; He, K.; Tang, H. Characteristics and formation mechanism of regional faults system in southern South China Sea and continental margins. *World Geol.* **2019**, *38*, 708–720. [CrossRef]
13. Xu, Z.; Li, Y.; Yan, W.; Lv, Y.; Zhang, G.; Lu, D.; Zhu, Z. Identifying submarine engineering geologic hazards in a potential gas hydrate target area on the southern continental margin of the South China Sea. *J. Mar. Sci. Eng.* **2022**, *10*, 2008. [CrossRef]
14. Hong, Z.; Meng, M.; Deng, K.; Bao, J.; Wang, Q.; Liu, X. A quick method for appraising pore connectivity and ultimate imbibed porosity in shale reservoirs. *J. Mar. Sci. Eng.* **2025**, *13*, 174. [CrossRef]
15. Han, B.; Zhao, Z.; Wang, X.; Sun, Z.; Li, F.; Zhu, B.; Yao, Y.; Liu, L.; Peng, T.; Long, G. Formation of the Zengmu and Beikang Basins, and West Baram Line in the southwestern South China Sea margin. *J. Oceanol. Limnol.* **2023**, *41*, 592–611. [CrossRef]
16. Luo, S.; Zhang, L.; Xu, G.; Xu, G.; Wang, X.; Lei, Z. The characteristics of the system domain and the stratigraphic framework of the Beikang-Zengmu Basin since the Middle Miocene. *Mar. Geol. Quat. Geol.* **2022**, *42*, 111–122. [CrossRef]
17. Tang, Z.; Xie, X.; Xu, J.; Wu, J.; Chen, B. Quantitative characterization of evolution and controlling factors of Paleo Rajang Delta in the Zengmu Basin. *J. Southwest Petrol. Univ. (Sci. Technol. Ed.)* **2025**, *47*, 147–162. [CrossRef]
18. Zheng, Q.L.; Li, S.Z.; Suo, Y.H.; Li, X.Y.; Guo, L.L.; Wang, P.C.; Zhang, Y.; Zang, Y.B.; Jiang, S.H.; Somerville, I.D. Structures around the Tinjar–West Baram Line in northern Kalimantan and seafloor spreading in the proto–South China Sea. *Geol. J.* **2016**, *51*, 513–523. [CrossRef]
19. Sun, J.L.; Zhang, Y.; Xu, H.; Cao, J. Cenozoic tectonics and basin evolution in the southwestern Nansha Sea area. *Earth Sci.* **2011**, *36*, 956–966.
20. Wang, Y.; Tu, G.; Yu, J.; Yan, P.; Jin, Y.; Chen, C.; Liu, J. Discovery of pockmarks in the Zengmu Basin, southern South China Sea and the implication. *J. Oceanol. Limnol.* **2023**, *41*, 757–768. [CrossRef]
21. Liu, S.; Hernández-Molina, F.J.; Lei, Z.; Duarte, D.; Chen, H.; Wang, C.; Lei, Y.; Zhuo, H.; Huang, S.; Zhang, L.; et al. Fault-controlled contourite drifts in the southern South China Sea: Tectonic, oceanographic, and conceptual implications. *Mar. Geol.* **2021**, *433*, 106420. [CrossRef]
22. Hong, Z.; Meng, M.; Y24uan, B.; Ma, C.; Wang, Q.; Deng, K.; Bao, J.; Yuan, M. Nanopore structure characterization of lacustrine and marine shales: Comparison between small angle neutron scattering and nitrogen adsorption methods. *Int. J. Hydrogen Energy* **2026**, *208*, 153565. [CrossRef]
23. Guo, C.; Tang, Y.; Fang, Y.; Wang, C.; Wei, X.; Li, H.; Chao, P.; Yang, T.; Song, Z.; Ren, J.; et al. Magmatism along the Nansha Trough on the southern continental margin of the South China Sea: Recent evidence from along-strike seismic profile. *Mar. Geol.* **2024**, *475*, 107344. [CrossRef]
24. Yu, J.; Yan, P.; Wang, Y.; Zhong, G.; Chen, C. Subsurface structures and nature of seafloor mounds in the northern South China Sea margin: Implications for Mesozoic hydrocarbon exploration. *Geomorphology* **2024**, *445*, 108973. [CrossRef]
25. Li, C.; Song, T. Magnetic recording of the Cenozoic oceanic crustal accretion and evolution of the South China Sea basin. *Chin. Sci. Bull.* **2012**, *57*, 3165–3181. [CrossRef]
26. Hakimi, M.H.; Abdullah, W.H.; Sia, S.G. Organic geochemical and petrographic characteristics of Tertiary coals in the northwest Sarawak, Malaysia: Implications for paleoenvironmental conditions and hydrocarbon generation potential. *Mar. Pet. Geol.* **2013**, *48*, 31–46. [CrossRef]

27. Chen, Y.; Zhang, S.; Li, J. Petroleum systems and source rock distribution in the Zengmu Basin, southern South China Sea. *Mar. Pet. Geol.* **2017**, *86*, 432–445. [CrossRef]
28. Xie, X.; Zhang, C.; Zhao, Z.; Liu, S.; Wang, L.; Lan, L.; Guo, J.; Wang, Y.; Song, S.; Bi, Y. Hydrocarbon geology, distribution and favourable exploration direction in Zengmu Basin, South China Sea. *China Offshore Oil Gas* **2015**, *27*, 19–26. Available online: https://m.book118.com/html/2015/0904/24667812.shtm (accessed on 11 February 2026).

Disclaimer/Publisher's Note: The statements, opinions and data contained in all publications are solely those of the individual author(s) and contributor(s) and not of MDPI and/or the editor(s). MDPI and/or the editor(s) disclaim responsibility for any injury to people or property resulting from any ideas, methods, instructions or products referred to in the content.